Role of Elastic Scattering in Electron Dynamics at Ordered Alkali Overlayers on Cu(111)

C. Corriol,[1] V. M. Silkin,[1] D. Sánchez-Portal,[1,2] A. Arnau,[1,2,3] E. V. Chulkov,[1,2,3] P. M. Echenique,[1,2,3] T. von Hofe,[4]
J. Kliewer,[4,*] J. Kröger,[4] and R. Berndt[4]

[1]*Donostia International Physics Center (DIPC), Paseo Manuel de Lardizabal 4, San Sebastian 20018, Spain*
[2]*Centro Mixto C.S.I.C.-UPV/EHU, Facultad de Química, Apartado 1072, San Sebastian 20080, Spain*
[3]*Departamento de Física de Materiales, Facultad de Química, Apartado 1072, San Sebastian 20080, Spain*
[4]*Institut für Experimentelle und Angewandte Physik, Christian-Albrechts-Universität zu Kiel, D-24098 Kiel, Germany*

Scanning tunneling spectroscopy of $p(2 \times 2)$ Cs and Na ordered overlayers on Cu(111) reveals similar
line widths of quasi-two-dimensional quantum well states despite largely different binding energies.
Detailed calculations show that 50% of the line widths are due to electron-phonon scattering while
inelastic electron-electron scattering is negligible. The mechanism of enhanced elastic scattering due to
Brillouin zone backfolding contributes the remaining width.

In many-electron systems ubiquitous interactions between quasiparticles such as electron-electron, electron-phonon or electron-magnon scattering are present and cause inelastic scattering. Elastic scattering is introduced by boundaries and defects such as, e.g., randomly placed adsorbates. The line shapes in electron spectroscopies are affected by these scattering processes and reflect the corresponding quasiparticle lifetimes. From an experimental point of view, electronic states which are localized at surfaces are directly accessible with photoelectron spectroscopies as well as scanning tunneling spectroscopy (STS). Consequently, these techniques are widely used to probe electron dynamics at surfaces [1–11].

An intringuing situation occurs when an extended *ordered* overlayer changes the periodicity of the surface. In reciprocal space, this corresponds to a mapping of the Brillouin zone of the pristine surface onto that of the overlayer (which is usually smaller) and results in backfolding of electronic bands. This can lead to closing of energy gaps in the surface Brillouin zone with drastic consequences for the electron dynamics at the interface.

Here, in a combined experimental and theoretical study, we analyze the processes that contribute to the width of quantum well states (QWS's) in Cs and Na overlayers on Cu(111). We achieve quantitative agreement between low temperature STS experiments and simulations of tunneling spectra using detailed calculations of the electronic structure of the surface and of the line width. The width of the QWS is shown to have significant contributions from the elastic width that appears as a result of the coupling to substrate states and from the inelastic electron-phonon scattering whereas inelastic electron-electron interaction is of minor importance.

For the present studies, STS offers the advantages of adequate energy resolution and the ability to identify defect-free surface areas. The lifetime broadening of surface states is extracted from STS measurements through a line shape analysis of conductance spectra [2]. Clean Cu(111) surfaces were prepared by standard Ar^+ bombardment and annealing cycles. Cs and Na were deposited from commercial dispensers (SAES Getters, Cologne, Germany) onto the sample at room temperature at rates of ≈ 0.5 ML min^{-1} as monitored with a quartz microbalance. We define one monolayer (ML) as one alkali atom per one Cu atom of the unreconstructed Cu(111) substrate. In the Cs case, a clear $p(2 \times 2)$ low-energy electron diffraction (LEED) pattern at room temperature [12,13] was used as additional indication of a 0.25 ML coverage. After preparation, samples were transferred to a scanning tunneling microscope (STM) and cooled to temperatures of 4.6–9 K. Spectroscopy of the differential conductance (dI/dV) was performed on homogeneous areas using a lock-in amplifier and adding a sinusoidal modulation (6 and 14 mV$_{pp}$ for Cs and Na, respectively) to the sample voltage. This results in an additional broadening [2] of the spectral feautures of 2.5 meV and 0.4 meV for Na and Cs, respectively. However, these values are comparable or smaller than the estimated experimental uncertainties of ± 3 and ± 2 meV for Na and Cs, respectively, and therefore we did not deconvolute the data.

Figure 1 displays dI/dV spectra (dots) of $p(2 \times 2)$ Cs and Na layers. Sharp rises of the conductance at $E_0 \cong 40$ meV and $E_0 \cong 410$ meV correspond to the minima of the quantum well state bands of Cs and Na overlayers, respectively. The width of the rise Δ, which is related to the inverse lifetimes of the these states [2], is similar in both cases. This observation is surprising in view of the large difference in binding energy which, in a simple picture, should cause widely different electron-electron (*e-e*) scattering. However, our calculations (solid lines in Fig. 1 and data in Table I) show that inelastic *e-e* scattering is unimportant. Electron-phonon (*e*-ph) scattering explains only 50% of the line widths, while enhanced elastic scattering, due to Brillouin zone backfolding, contributes the missing 50%.
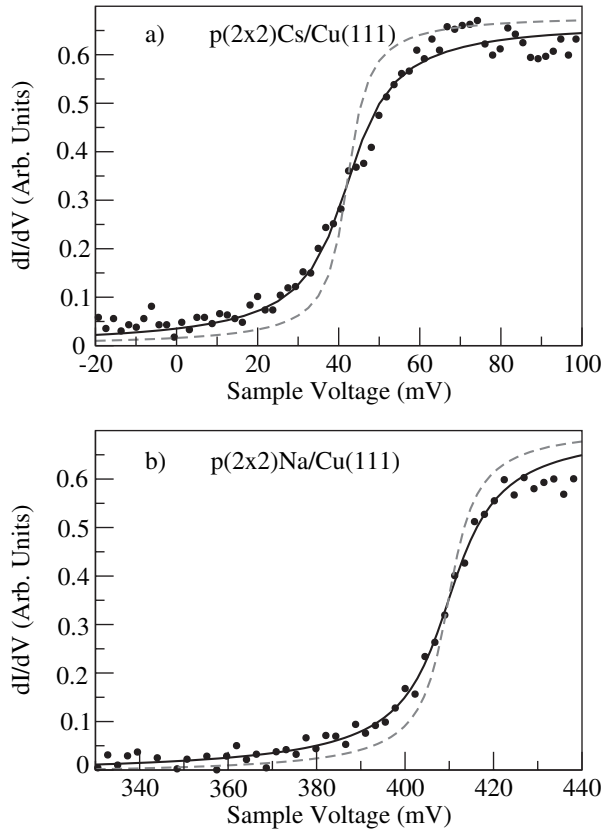
176802-1

FIG. 1.　Comparison between measured (dots) and calculated (lines) dI/dV curves for $p(2 \times 2)$ structures of (a) Cs and (b) Na on Cu(111). The solid lines include both the elastic and inelastic contributions to the energy width, while the dashed lines include only the inelastic one.

The surface electronic structure of both systems has been calculated using the density functional code VASP [14]. These slab calculations provide the input structures for the recursive calculation of the elastic width in the semi-infinite medium, as described below. Projected augmented waves [15] are used to describe the ionic cores and a plane wave basis set for the valence electrons. The exchange and correlation potential is treated in the generalized gradient approximation [16]. We have checked the convergency of the calculations with respect to the thickness of the slab up to 10 layers of Cu. A k sampling containing 14 inequivalent points was used for the self-

TABLE I.　Linewidth contributions (in meV) of various scattering channels: $\Gamma_{elastic}$ elastic, Γ_{e-e} electron-electron, and Γ_{e-ph} electron-phonon scattering. Γ_{total} is the resulting total width. Experimental estimates $\tilde{\Gamma}$ are determined from the width of the rise Δ in dI/dV spectra as explained in the text.

	$\Gamma_{elastic}$	Γ_{e-e}	Γ_{e-ph}	Γ_{total}	$\tilde{\Gamma}$
Cs	9.4	<0.1	7.5 ± 3	17 ± 3	18 ± 2
Na	7.4	0.4	9 ± 3	16.8 ± 3	16 ± 3

consistent calculations of the (2×2) superstructures. A finer sampling, with up to 154 inequivalent points, was used for the simulations of the tunneling spectra in order to achieve the required energy resolution. The tunneling conductance is calculated with a model that assumes a smooth density of states of the tip around the Fermi level. Then, at small positive sample bias, the energy dependence of the conductance is determined by the sample density of states [17]. The details of the model are described elsewhere [18]. In brief, we introduce an energy width ($\Gamma_m/2$) of the states when calculating the imaginary part of the surface Green function, i.e., the surface local density of states (LDOS). This width corresponds to a Lorentzian weight for each state such that the surface LDOS is given by

$$\rho(\varepsilon, \vec{r}) = \frac{1}{\pi} \sum_m |\Psi_m(\vec{r})|^2 \frac{\Gamma_m/2}{(\varepsilon - \varepsilon_m)^2 + (\Gamma_m/2)^2}. \quad (1)$$

The eigenvalues (ε_m) and eigenfunctions (Ψ_m) are taken from VASP, while the energy width ($\Gamma_m/2$) is determined as described below. The sum over m includes both a summation over the band index and an integration over parallel momentum. The LDOS is calculated at 3 Å from the alkali overlayer, where the electronic corrugation is negligible, and it is dominated by the QWS band in the relevant energy range.

For comparing the measured dI/dV data for the $p(2 \times 2)$ Cs structure on Cu(111) and the simulated spectrum we return to Fig. 1(a). No fitting parameter has been used apart from a scaling factor for the calculated conductance. The agreement between the data points and the solid curve clearly shows the importance of the elastic width in determining the shape of the spectrum at the onset around 40 meV. Figure 1(b) displays a similar comparison for a $p(2 \times 2)$ Na film on Cu(111). In this case, the calculated curves have been shifted by +18 meV to match the experimental binding energy [19]. The shape of the curve at the onset also agrees well with the measured data in this case.

The adsorption of alkali adlayers in $p(2 \times 2)$ superstructures leads to a modification of the projected bulk band structure of the substrate as shown in Fig. 2 along the $\bar{\Gamma}$-$\bar{M}$ direction. The inset displays the surface Brillouin zones (SBZ's) for a $p(2 \times 2)$ overlayer and for a (1×1) substrate. In the overlayer case the energy gap near E_F of clean Cu(111) surface is closed due to the folding of bands originally situated along the $\bar{M}$-$\bar{M}_{Cu}$ and $\bar{M}_{Cu}$-$\bar{K}'$ symmetry directions onto the $\bar{\Gamma}$-$\bar{M}$ direction. The corresponding extra corrugation of the Cu(111) surface due to the coupling between the $p(2 \times 2)$ adsorbate layer and underlying Cu bulk states causes some mixing of the alkali induced QWS at $\bar{\Gamma}$ and substrate Cu states at the $\bar{M}_{Cu}$ point of the (1×1) Brillouin zone. This serves as a source of elastic scattering, which requires a quantitative analysis.

To calculate the elastic width of QWS's we compute the Green function of the combined system (adlayer plus
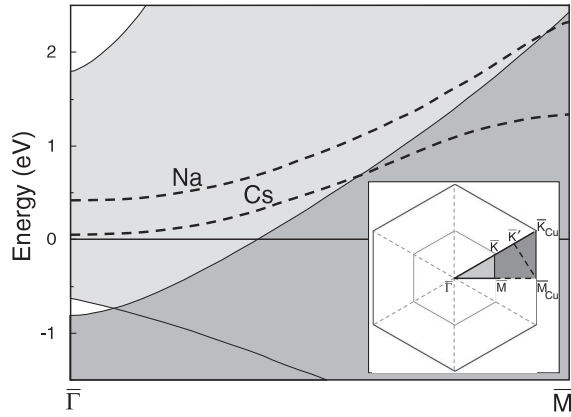
FIG. 2. Dispersion of $p(2 \times 2)$ Na and Cs quantum well states in the $\bar{\Gamma}$-$\bar{M}$ direction. Dark gray indicates bulk Cu states of the (1×1) SBZ, while light gray shows the closing of the gap around $\bar{\Gamma}$ after backfolding from the $\bar{M}$-$\bar{M}_{Cu}$ and $\bar{M}_{Cu}$-$\bar{K}'$ directions onto $\bar{\Gamma}$-$\bar{M}$ defined in the inset.

semi-infinite substrate) with high precision in the surface region. A localized basis set greatly simplifies this calculation, which is performed using recursive techniques. We, therefore, use the SIESTA code [20], which utilizes a basis set of numerical atomic orbitals [21]. The results for the electronic structure are almost identical to those obtained with VASP. With this local basis set the elements of the Hamiltonian and overlap matrices between atoms that are far apart (beyond ≈ 15 Å in our case) are strictly zero. The infinite system can now be divided in groups of layers ("slices") that only interact with the nearest neighbor groups. The Hamiltonian matrix elements (H_{jk}) and overlaps (S_{jk}) for orbitals in the surface slice, and its interaction with orbitals in underlying layers, are obtained from the slab calculation. The interactions in the inner slices are taken from a calculation of bulk Cu. A common energy reference is set by aligning the Fermi levels of both calculations. We now use the recursive relation

$$G^{ij}(\omega, \mathbf{k}_{\|})[H_{jk}(\mathbf{k}_{\|}) - \omega S_{jk}(\mathbf{k}_{\|})] = \delta^i_k \qquad (2)$$

to obtain the Green function in the surface region. We use a method similar to that described in Ref. [22] to iteratively solve this equation. The matrix elements are defined such that $G(\mathbf{r}, \mathbf{r}'; \omega, \mathbf{k}_{\|}) = G^{ij}(\omega, \mathbf{k}_{\|})\phi_i(\mathbf{r})\phi_j(\mathbf{r}')$, where the ϕ_i are the atomic orbitals and the sum over repeated indices is assumed. Our strategy is then to project the Green function onto a wave packet Ψ_R localized in the surface region. The function $\text{Im}\{\langle\Psi_R|\hat{G}(\omega)|\Psi_R\rangle\}$ exhibits well-defined peaks at energies ϵ_R corresponding to the QWS of the overlayer. The shape and position of these peaks are independent of the selection of Ψ_R, as far as Ψ_R has predominant contributions from the orbitals in the adsorbates. The peaks have a Lorentzian shape with a width and position that can be easily extracted using a least square fit [23]. Carrying out this procedure for the two systems studied here we find

values of the elastic width at $\bar{\Gamma}$ equal to 9.4 meV and 7.4 meV for Cs and Na systems, respectively. The parallel momentum dependence of the elastic width is rather weak and does not introduce significant changes in the shape of the calculated dI/dV spectra.

For both systems of interest we estimate the inelastic e-e contribution (Γ_{e-e}) to the QWS linewidth by using a model in which the one-electron potential is constant in a plane parallel to the surface and varies only in the direction z perpendicular to the surface. We use here the parametrized potential proposed in Ref. [24] for thin films adsorbed on Cu(111). The parameters are fitted to reproduce the energy E_0 of the QWS and the first image potential state energy E_1. For E_0 we take the values 42 meV and 408 meV for Cs and Na, respectively, from the dI/dV curves. As E_1 is not known, we take $E_1 = -0.60$ eV (with respect to the vacuum level) for both systems. The variation of E_1 from -0.50 to -0.75 eV does not affect our conclusion on inelastic Γ_{e-e} contribution to the linewidth since the image state is well separated in energy and in space from the QWS. Γ_{e-e} is calculated within the GW approximation [6] by employing eigenfunctions and eigenenergies obtained with this model potential. The computed Γ_{e-e} values of less than 0.1 and 0.4 meV in the Cs and Na systems, respectively, demonstrate that inelastic e-e scattering provides only a small contribution to the QWS linewidth. This latter fact reflects the difference between electrons and holes; for electrons at the bottom of the QWS band the intraband channel is completely absent, while it is most important for holes [4].

Another inelastic contribution, the e-ph one, is found to be important for the studied systems. As there is no information on phonon dispersion in these systems, we make two kinds of approximations to estimate this contribution. First, we assume that the low frequency phonon spectrum can be approximated by that of other system with similar coverage on different surface orientations. Second, we estimate the e-ph coupling constant λ within reasonable uncertainty limits. For $p(2 \times 2)$ Cs/Cu(111) we use the phonon dispersion data for a monolayer of Cs on Cu(100) [25] which revealed a Cs induced flat optical mode around the $\bar{\Gamma}$ point with $\hbar\omega \approx 7.5$ meV and two Cs induced acoustic modes with $\hbar\omega = 6$ and 5 meV at the zone boundary. Using the Einstein model [26] to treat a flat optical phonon mode and 2- and 3-dimensional Debye models [24] for the two acoustic modes, as well as a value of $\lambda = 0.18$, we estimate $\Gamma_{e-ph} = 7.5 \pm 3$ meV for $p(2 \times 2)$ Cs/Cu(111). This value coincides with the maximum value $\lambda = 0.15 \pm 0.03$ in bulk Cs [26]. The error bar ± 0.06 covers the range from the minimum bulk value $\lambda = 0.12$ to the value $\lambda = 0.24$ for a monolayer of Na on Cu(111) [27]. The former error bar also covers the results obtained with different Debye models. For Na on Cu we also assume that the measured maximum phonon frequency for a monolayer of Na on Cu(100) can be applied

to $p(2 \times 2)$ Na/Cu(111). Following Ref. [24] we use $\lambda = 0.24$ and Debye energy $\hbar\omega_D = 18$ meV yielding $\Gamma_{e-ph} = 9.0 \pm 3$ meV.

An overview of the different contributions to the line width of the QWS at the $\bar{\Gamma}$ point is presented in Table I. The elastic contribution to the energy width accounts for approximately 50% of the total width. The inelastic e-ph contribution is comparable. However, the inelastic e-e contribution is negligible. While experimental and calculated dI/dV spectra are compared directly in Fig. 1 experimental estimates $\tilde{\Gamma}$ of the linewidth can also be obtained from the width of the rise Δ in the spectra using the approximate relation $\tilde{\Gamma} = (2/\pi)\Delta$.

In summary, our combined experimental and theoretical study shows that the dynamics of electrons at ordered alkali overlayers on noble metal surfaces is determined by the elastic width due to the coupling to the bulk continuum and by inelastic e-ph scattering. However, inelastic e-e scattering does not play a role. The relative importance of the elastic contribution for other ordered superstructures will depend on details like the density of states at given points of the substrate SBZ. Any change of periodicity in going from the surface to the overlayer structure will lead to a modification of the scattering channels that determine the dynamics of electrons at the interface.

---

*Present address: Infineon Technologies AG, D-81609 München, Germany.

[1] H. Petek and S. Ogawa, Prog. Surf. Sci. **56,** 239 (1997).

[2] J. Li, W. D. Schneider, R. Berndt, O. R. Bryant, and S. Crampin, Phys. Rev. Lett. **81,** 4464 (1998).

[3] L. Bürgi, O. Jeandupeux, H. Brune, and K. Kern, Phys. Rev. Lett. **82,** 4516 (1999).

[4] J. Kliewer, R. Berndt, E. V. Chulkov, V. M. Silkin, P. M. Echenique, and S. Crampin, Science **288,** 1399 (2000).

[5] K. F. Braun and K. H. Rieder, Phys. Rev. Lett. **88,** 096801 (2002).

[6] P. M. Echenique, R. Berndt, E. V. Chulkov, Th. Fauster, A. Goldmann, and U. Höfer, Surf. Sci. Rep. **52,** 219 (2004).

[7] K. Boger, M. Weinelt, and Th. Fauster, Phys. Rev. Lett. **92,** 126803 (2004).

[8] D. Wegner, A. Bauer, and G. Kaindl, Phys. Rev. Lett. **94,** 126804 (2005).

[9] L. Limot, E. Pehlke, J. Kröger, and R. Berndt, Phys. Rev. Lett. **94,** 036805 (2005).

[10] H. Jensen, J. Kröger, R. Berndt, and S. Crampin [Phys. Rev. B (to be published)].

[11] S. Crampin, J. Kröger, H. Jensen, and R. Berndt, Phys. Rev. Lett. **95,** 029701 (2005).

[12] S. Å. Lindgren, L. Walldén, J. Rundgren, P. Westrin, and J. Neve, Phys. Rev. B **28,** 6707 (1983).

[13] R. D. Diehl and R. McGrath, Surf. Sci. Rep. **23,** 43 (1996).

[14] G. Kresse and J. Hafner, Phys. Rev. B **47,** 558 (1993); **49,** 14 251 (1994); G. Kresse and J. Furthmüller, Comput. Mater. Sci. **6,** 15 (1996); Phys. Rev. B **54,** 11 169 (1996).

[15] P. E. Blöchl, Phys. Rev. B **50,** 17 953 (1994).

[16] J. P. Perdew, K. Burke, and Y. Wang, Phys. Rev. B **54,** 16 533 (1996).

[17] A. Partridge, G. J. Tatlock, F. M. Leibsle, C. F. J. Flipse, G. Hörmandiger, and J. B. Pendry, Phys. Rev. B **48,** 8267 (1993).

[18] C. Corriol, A. Arnau, V. M. Silkin, E. V. Chulkov, and P. M. Echenique (to be published).

[19] This shift is consistent with the expected accuracy of density functional calculations. See J. M. Carlsson and B. Hellsing, Phys. Rev. B **61,** 13 973 (2000).

[20] J. M. Soler, E. Artacho, J. D. Gale, A. García, J. Junquera, and D. Sánchez-Portal, J. Phys. Condens. Matter **14,** 2745 (2002).

[21] We have used a double-ζ polarized basis sets of pseudo-atomic orbitals. The radii of the orbitals for Cu were fixed with an energy shift [20] of 200 meV. The basis set of Cs and Na corresponds to $a + 1$ ionic configuration, and the orbital radii were fixed, respectively, to 9 and 8 Bohrs. For Cs the $5p$ electrons were included explicitly in the calculations.

[22] E. Artacho and F. Yndurain, Phys. Rev. B **44,** 6169 (1991).

[23] We perform a fit to $[(\omega - \epsilon_R)^2 + (\Gamma_R/2)^2]^{-1}$ in the energy range of interest. In order to obtain convergence of the iterative solution of Eq. (2) it is necessary to evaluate the Green function outside the real axis. To this end, a small imaginary part is added to the energy $\omega + i\delta$. To estimate the physical (elastic) width $\Gamma_{elastic}$ of the QWS, this artificial width is substracted from the fitted value Γ_R. We have thus $\Gamma_{elastic} = \Gamma_R - 2\delta$. We have used three different values of δ, (1.0, 0.5, and 0.25 meV), obtaining identical values for $\Gamma_{elastic}$ within ≈ 0.1 meV.

[24] E. V. Chulkov, J. Kliewer, R. Berndt, V. M. Silkin, B. Hellsing, S. Crampin, and P. M. Echenique, Phys. Rev. B **68,** 195422 (2003).

[25] G. Witte and J. P. Toennies, Phys. Rev. B **62,** R7771 (2000).

[26] G. Grimvall, in *The Electron-Phonon Interaction in Metals, Selected Topics in Solid State Physics*, edited by E. Wohlfarth (North-Holland, New York, 1981).

[27] B. Hellsing, J. Carlsson, L. Wallden, and S. A. Lindgren, Phys. Rev. B **61,** 2343 (2000).